

In-band OSNR monitoring using a pair of Michelson fiber interferometers

E. Flood^{1*}, W. H. Guo¹, D. Reid², M. Lynch¹, A. L. Bradley¹, L. P. Barry², and J. F. Donegan¹

¹*Semiconductor Photonics Group, School of Physics, Trinity College, Dublin 2, Ireland*

²*Research Institute for Networks and Communications Engineering, Dublin City University, Dublin 9, Ireland*
**flood@tcd.ie*

Abstract: Two polarization-independent Michelson fiber interferometers with different optical delays were used to measure the in-band OSNR of an optical signal from 5 to 30dB within an accuracy of 0.5dB. Using an expansion of the amplitude autocorrelation function of the signal around zero delay, it was possible to perform measurements without any prior knowledge of the signal. The system is shown to be immune to the effects of modulation frequency (up to 10G), partially and fully polarized noise, chromatic dispersion and poorly biased modulators.

©2010 Optical Society of America

OCIS codes: (060.2330) Fiber optics communications; (120.3180) Interferometry.

References and links

1. D. C. Kilper, R. Bach, D. J. Blumenthal, D. Einstein, T. Landolsi, L. Ostar, M. Preiss, and A. E. Willner, "Optical Performance Monitoring," *J. Lightwave Technol.* **22**(1), 294–304 (2004).
2. H. Suzuki, and N. Takachio, "Optical signal quality monitor built into WDM linear repeaters using semiconductor arrayed waveguide grating filter monolithically integrated with eight photodiodes," *Electron. Lett.* **35**(10), 836–837 (1999).
3. J. H. Lee, H. Y. Choi, S. K. Shin, and Y. C. Chung, "A Review of the Polarization-Nulling Technique for Monitoring Optical-Signal-to-Noise Ratio in Dynamic WDM Networks," *J. Lightwave Technol.* **24**(11), 4162–4171 (2006).
4. C. Xie, D. C. Kilper, L. Moller, and R. Ryf, "Orthogonal-Polarization Heterodyne OSNR Monitoring Insensitive to Polarization-Mode Dispersion and Nonlinear Polarization Scattering," *J. Lightwave Technol.* **25**(1), 177–183 (2007).
5. Z. Tao, Z. Chen, L. Fu, D. Wu, and A. Xu, "Monitoring of OSNR by using a Mach-Zehnder interferometer," *Microw. Opt. Technol. Lett.* **30**(1), 63–65 (2001).
6. Y. K. Lizé, J. Y. Yang, L. Christen, X. Wu, S. Nuccio, T. Wu, A. E. Willner, R. Kashyap, and F. Séguin, "Simultaneous and Independent Monitoring of OSNR, Chromatic and Polarization Mode Dispersion for NRZ-OOK, DPSK and Duobinary," in *Optical Fiber Communication Conference and Exposition and The National Fiber Optic Engineers Conference*, OSA Technical Digest Series (CD) (Optical Society of America, 2007), paper OThN2.
7. X. Liu, Y.-H. Kao, S. Chandrasekhar, I. Kang, S. Cabot, and L. L. Buhl, "OSNR Monitoring Method for OOK and DPSK Based on Optical Delay Interferometer," *IEEE Photon. Technol. Lett.* **19**(15), 1172–1174 (2007).
8. J. M. Oh, M. Brodsky, L. E. Nelson, G. Cadena, and M. D. Feuer, "Interferometric optical signal-to-noise ratio measurements of telecom signals with degraded extinction ratio," *Opt. Lett.* **33**(18), 2065–2067 (2008).
9. A. D. Kersey, M. J. Marrone, and M. A. Davis, "Polarisation-insensitive fibre optic Michelson interferometer," *Electron. Lett.* **27**(6), 518–520 (1991).

1. Introduction

In order to realize next generation communications networks, it will be essential to implement performance monitoring in the optical layer. Currently, monitoring is realized through use of optical/electrical/optical devices, which will be impossible for the case of a transparent DWDM network. Several diagnostics of the optical signal will be required to meet this monitoring need, one of which is optical signal to noise ratio (OSNR) monitoring.

The cascading of optical amplifiers in communications networks causes the accumulation of amplified spontaneous emission (ASE) noise, which is one of the main impairments in optical networks. ASE noise is typically quantified by the optical-signal-to-noise-ratio (OSNR), which is measured within an optical bandwidth of 0.1 nm. Due to its influence on

the bit-error-rate of an optical signal, its role in fault diagnosis and as a measure of general network health, it is important to have a reliable means of OSNR monitoring over a large range of signal and noise [1]

Current methods involve measuring the noise at some offset from the centre frequency of a channel and performing a linear interpolation in order to make an estimate of the in-band OSNR [2]. This technique becomes unreliable with the use of reconfigurable optical add-drop multiplexers (ROADM). Due to the presence of channels with vastly different transmission histories, an inter-channel OSNR measurement becomes unreliable. In order to elucidate any meaningful result, a direct measurement of the in-band OSNR is necessary.

Several in-band OSNR measurement techniques have been proposed, one example of which is the polarization nulling method. This technique relies on the assumption that the signal is completely polarized while the noise is completely unpolarized [3]. In practice, the presence of polarized noise due to polarization dependent loss in the fiber and depolarized signal as a result of polarization mode dispersion (PMD) and nonlinear polarization scattering makes the measurement less reliable. The use of orthogonal polarization heterodyne mixing has also been proposed and, while it is impervious to the effects of PMD, it relies on the assumption of completely unpolarized noise [4].

It is possible to overcome these issues by employing a Mach-Zehnder (MZ) interferometer to exploit the coherence difference between signal and noise by modulating the phase of one arm of the interferometer and using the extinction ratio due to the interference in the two arms to calculate the OSNR. Such a system has been shown to be immune to the effects of partially polarized noise, PMD-induced signal depolarization, chromatic dispersion, bit-rate, modulation format and capable of measuring OSNR values exceeding 30 dB for OOK and PSK signals [5–7]. These systems have been shown to be relatively cheap and reliable but the proposed single-interferometer schemes are not without disadvantages. In order to operate such a device one must have prior knowledge of the amplitude autocorrelation (AAC) function of the signal. In the case of the above method, this quantity can only be measured by “turning off” the noise, scanning the signal interference and using the resultant value as the signal AAC in subsequent calculations. Such a procedure is unrealistic for practical usage due to the effect of modulator bias on the signal AAC [8].

In this paper, we present a method which, like the aforementioned interferometer-based examples, is based on exploiting the coherence difference between signal and ASE. This retains the advantages of such systems but dispenses with the requirement of knowing the AAC of the signal. The technique is insensitive to the input polarization, devoid of free-space elements and can measure the OSNR over a similar dynamic range. This can be achieved by using a double Michelson fiber interferometer scheme with adjustable phase delay and different optical delays that are much smaller than the bit period of the signal and may be still within the coherence time of the noise, which is determined by the transmission function of the channel filter.

Operating principle

Figure 1(a) shows the OSNR monitor setup. The interferometers each consist of two 3 dB couplers and two Faraday rotator mirrors. The effect of the Faraday mirrors is to impose a 45 degree single pass polarization rotation, effectively “unwinding” the polarization change in the fiber [9]. This removed the necessity for dynamic polarization control in the device and should allow accurate OSNR measurements to be performed on polarization multiplexed signals. One arm of each interferometer has a fixed optical delay of the order of ps. These delays were measured by scanning the interferometers’ transmission as a function of wavelength and calculating the delay from the free-spectral range. The delays can be set by using different combinations of fiber couplers as their magnitudes are of the order of the manufacturing tolerance of the fibers (approx 1mm) and were characterized as 8 ps and 17 ps. The other arm of each interferometer had a variable phase element (basically another delay element but of the order of fs), which adjusted the phase in each arm over multiples of π by stretching the fibers using a piezoelectric (PZ) tube. High sensitivity, low speed photodiodes

(PD) record the transmitted intensity and the information is acquired using the analogue input of a data acquisition card (DAQ) which measures a dependence as shown in Fig. 1(b). The extinction ratio of this plot is the ratio of the maximum to the minimum transmitted voltage, $\rho = V_{\max}/V_{\min}$ and may be used to calculate the OSNR by methods described in the next section.

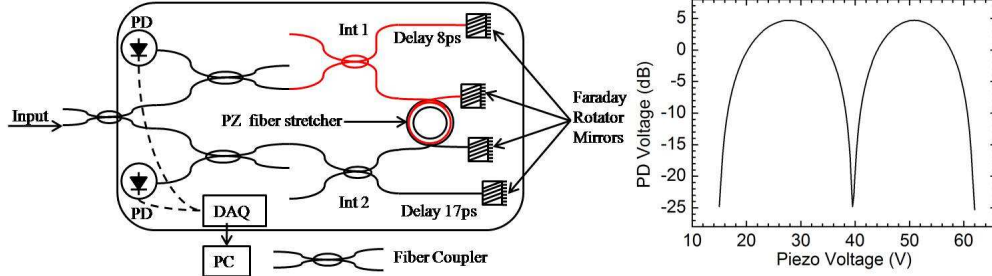


Fig. 1. (a) Interferometer setup, PD: photodiode, PZ: Piezo crystal; Int1 and 2: interferometers; (b) Interferometer transmission.

Theory

The signal after the channel filter can be expressed as $e_{in}(t) = E(t) \exp(j2\pi f_0 t)$, where f_0 is the carrier frequency. After the interferometer the signal is described by Eq. (1).

$$e_{out}(t) = \sqrt{K_d} E(t + \tau_d) \exp(j2\pi f_0 (t + \tau_d)) + \sqrt{K_p} E(t + \tau_p) \exp(j2\pi f_0 (t + \tau_p)) \quad (1)$$

where K_d represents the power of the signal passing through the interferometer arm with the optical delay and K_p represents the power of the signal passing through the interferometer arm with the variable optical phase, τ_d is the delay which is of the order of ps and τ_p is for the phase adjustment which of the order of the optical cycle (~ 5 fs). For noise we can use similar expressions. The noise immediately after the channel filter can be expressed as $n_{in}(t) = N(t) \exp(j2\pi f_0 t)$. After the interferometer it will be expressed as Eq. (2)

$$n_{out}(t) = \sqrt{K_d} N(t + \tau_d) \exp(j2\pi f_0 (t + \tau_d)) + \sqrt{K_p} N(t + \tau_p) \exp(j2\pi f_0 (t + \tau_p)) \quad (2)$$

We assume the interferometer is polarization insensitive so we adopt a scalar description of the signal and the noise. The low speed photodiode will detect a voltage as in Eq. (3)

$$V = C |e_{out}(t) + n_{out}(t)|^2 \quad (3)$$

where C is a constant relating to the detector efficiency. The noise may be expressed as in Eq. (4)

$$\begin{aligned} \overline{N(t)} &= 0, \overline{N^*(t)N(t)} = P_n \\ \overline{N^*(t)N(t+\tau)} &= \int F(f) \exp(j2\pi f \tau) df \\ \overline{N(t)N^*(t+\tau)} &= \int F(-f) \exp(j2\pi f \tau) df \\ \int \frac{F(f) + F(-f)}{2} \exp(j2\pi f \tau) df &\equiv \gamma_n(\tau) P_n \end{aligned} \quad (4)$$

where $F(f)$ is the noise power spectrum, P_n is the noise average power. If the noise power spectrum is simply determined by the power transmission function of the channel filter which can be accurately measured, γ_n , the autocorrelation of the noise amplitude, can be determined through its definition in Eq. (4). In the event that the signal has passed through many

ROADMs before reaching the channel filter, the noise power spectrum will not simply be determined by the power transmission function of the channel filter. In this situation we think it is possible to turn off the signal and measure the interferogram visibility of the noise which will still be present due to the cascaded fibre amplifiers. γ_n can then be obtained from the measured visibility through the following Eq. (12) (when $r \rightarrow \infty$, $\gamma_n = M$). In the following analysis we assume γ_n has been known. As seen from (4), γ_n will be a real and even function of the delay τ and will have a peak value of 1 at $\tau = 0$.

The signal after the channel filter may be defined as in Eq. (5)

$$\begin{aligned} \overline{E^*(t)E(t)} &= P_s \\ \overline{E^*(t)E(t+\tau)} &= \int S(f) \exp(j2\pi f \tau) df \\ \overline{E(t)E^*(t+\tau)} &= \int S(-f) \exp(j2\pi f \tau) df \\ \int \frac{S(f)+S(-f)}{2} \exp(j2\pi f \tau) df &\equiv \gamma_s(\tau)P_s \end{aligned} \quad (5)$$

where $S(f)$ is the signal power spectrum, P_s is the signal average power. As seen from (5), $\gamma_s(\tau_d)$, the autocorrelation of the signal amplitude will be a real and even function of τ_d as well and will always have a peak value of 1 at $\tau_d = 0$.

With the above definition, the voltage detected can be simplified as in Eq. (6)

$$V = C \left[\begin{aligned} &(\mathbf{K}_d + \mathbf{K}_p)(P_s + P_n) + 2\sqrt{\mathbf{K}_d \mathbf{K}_p} \\ &\times \cos(2\pi f_0(\tau_d - \tau_p)) (P_s \gamma_s(\tau_d - \tau_p) + P_n \gamma_n(\tau_d - \tau_p)) \end{aligned} \right] \quad (6)$$

Because $\tau_p \ll \tau_d$, the Eq. (6) can be further simplified to give Eq. (7)

$$\begin{aligned} V &= C[(\mathbf{K}_d + \mathbf{K}_p)(P_s + P_n) + 2\sqrt{\mathbf{K}_d \mathbf{K}_p} \\ &\times \cos(2\pi f_0(\tau_d - \tau_p)) (P_s \gamma_s(\tau_d) + P_n \gamma_n(\tau_d))] \end{aligned} \quad (7)$$

For each τ_d with changing τ_p , the current will follow a sine curve which is the interferogram of the noisy signal. The interferogram has maximum and minimum value as in Eqs. (8) and (9) respectively

$$V_{\max} = C \left[(\mathbf{K}_d + \mathbf{K}_p)(P_s + P_n) + 2\sqrt{\mathbf{K}_d \mathbf{K}_p} (P_s \gamma_s(\tau_d) + P_n \gamma_n(\tau_d)) \right] \quad (8)$$

$$V_{\min} = C \left[(\mathbf{K}_d + \mathbf{K}_p)(P_s + P_n) - 2\sqrt{\mathbf{K}_d \mathbf{K}_p} (P_s \gamma_s(\tau_d) + P_n \gamma_n(\tau_d)) \right] \quad (9)$$

The extinction of the interferogram is $\rho = V_{\max}/V_{\min}$ which is the main quantity we need to measure in the proposed scheme. In practice the extinction is always expressed on the log scale because it is generally a large value. From the maximum and minimum values of the interferogram we can define the quantities V_{ave} and V_{diff} as in Eqs. (10) and (11) respectively

$$V_{ave} \equiv \frac{V_{\max} + V_{\min}}{2} = C(\mathbf{K}_d + \mathbf{K}_p)(P_s + P_n) \quad (10)$$

$$V_{diff} \equiv \frac{V_{\max} - V_{\min}}{2} = 2C\sqrt{\mathbf{K}_d \mathbf{K}_p} (P_s \gamma_s(\tau_d) + P_n \gamma_n(\tau_d)) \quad (11)$$

The visibility of the interferogram is defined as $\mu = V_{diff}/V_{ave}$. The visibility and extinction of an interferogram are related to each other simply through $\mu = (\rho-1)/(\rho+1)$ and $\rho = (1+\mu)/(1-\mu)$. So we can notice that if the visibility is close to 1 for example 0.998, the extinction would be very high for example close to 1000 (30 dB). We define $r \equiv P_n/P_s$ which leads to Eq. (12)

$$\frac{\gamma_s(\tau_d) + r\gamma_n(\tau_d)}{1+r} = \frac{V_{\text{diff}}(K_d + K_p)}{V_{\text{ave}} 2\sqrt{K_d K_p}} = \frac{\mu}{\left(\frac{2\sqrt{K_d K_p}}{(K_d + K_p)}\right)} \equiv M \quad (12)$$

where M is the interferogram visibility of the noisy signal when the optical power imbalance in each arm of the interferometer has been addressed. r is then given by Eq. (13)

$$r = \frac{\gamma_s(\tau_d) - M}{M - \gamma_n(\tau_d)} \quad (13)$$

As stated above $\gamma_n(\tau_d)$ is known, so if $\gamma_s(\tau_d)$ is known then the signal to noise ratio can be found and the OSNR can therefore be derived as in Eq. (14)

$$\text{OSNR} = 10 \log_{10} \left(\frac{\text{NEB}(\text{nm})}{r \times 0.1(\text{nm})} \right) = -10 \log_{10}(r) + 10 \log_{10} \left(\frac{\text{NEB}(\text{nm})}{0.1(\text{nm})} \right) \quad (14)$$

where NEB is the noise equivalent bandwidth of the channel filter. For the methods that are already developed based on a single interferometer with a fixed optical delay, the delay between the two arms is always made large enough to ensure $\gamma_n(\tau_d)$ is approximately zero. $\gamma_s(\tau_d)$ is obtained by turning off the noise source, in which case only signal is present so $r = 0$ and $\gamma_s(\tau_d) = M$ can be measured directly as from Eq. (12). After the noise is added, the same $\gamma_s(\tau_d)$ is used to obtain the OSNR. This method is shown to be immune to various impairments such as depolarization of the signal caused by polarization mode dispersion (PMD) and partial polarization of the noise caused by polarization dependent loss (PDL) of optical elements installed in the optical link. One problem is that practically it is difficult to turn off the noise because in a long optical link the fibre amplifiers have to be there so the signal will always accumulate additional noise. For this reason it is difficult to obtain $\gamma_s(\tau_d)$. Furthermore, $\gamma_s(\tau_d)$ could change because the DC bias or the drive signal of the modulator used to generate the signal could change. Additional filtering and self (cross) phase modulation which change the signal spectrum could also change $\gamma_s(\tau_d)$. So the signal amplitude autocorrelation should be periodically monitored, which is difficult for a single interferometer with a fixed optical delay.

Observing the function of $\gamma_s(\tau_d)$, we can find that it always has a nearly parabolic shape around the zero delay. So if we employ optical delays much less than the bit period $1/\nu$, where ν is the frequency of the signal, we can expand $\gamma_s(\tau_d)$ around $\tau_d = 0$ as in Eq. (15)

$$\gamma_s(\tau_d) = 1 - \sum_{k=1}^K c_k \tau_d^{2k}. \quad (15)$$

We just have terms with powers of $2k$ in (15) because as pointed out above $\gamma_s(\tau_d)$ is an even function of τ_d . Using this relation we can change Eq. (13) into Eq. (16).

$$\sum_{k=1}^K c_k \tau_{d,q}^{2k} + r(M_q - \gamma_n(\tau_{d,q})) = 1 - M_q \quad (16)$$

where the subscript q means we have made a series of measurements with different delays represented by $\tau_{d,q}$ where q is from 1 to Q . So Eq. (16) represents a series of linear equations with unknown values of r and c_k which can be solved if $Q \geq K + 1$. Generally selecting $k = 1$ and doing two measurements at two different delays, i.e. $Q = 2$, can achieve results within the appropriate range and accuracy (30dB \pm 0.5dB OSNR). In the following description we generally assume that we measure two interferograms of the noisy signal at two different delays which are small compared with the bit period (100 ps for a 10G signal).

Results

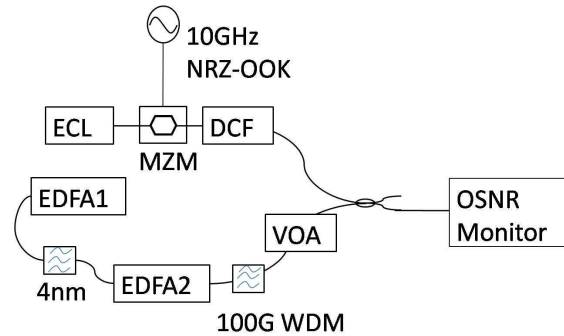


Fig. 2. OSNR monitoring setup

The experimental setup is shown in Fig. 2. A signal was provided by an external cavity tunable laser tuned to 1549.4nm and modulated by a 10G non-return to zero on-off keyed (NRZ-OOK) pseudo-random bit sequence (PRBS) through a Mach-Zehnder modulator (MZM). 600ps/nm of chromatic dispersion was imposed by a dispersion compensation fiber (DCF) after the modulator. Noise was provided by two Erbium doped fiber amplifiers (EDFA1 and EDFA2) cascaded together, with the output of EDFA1 filtered to 4 nm and used as the input for EDFA2. The output of EDFA2 was filtered using a 100G DWDM filter (NEB = 0.6 nm). This was combined with the signal using a 3 dB coupler and fed into the input of our OSNR monitor. The OSNR was changed by attenuating the noise power using a variable optical attenuator while keeping the signal power constant. The reference OSNR was measured initially using a power meter. The piezoelectric tube was oscillated at a low frequency (~1 Hz) and it was possible to measure the photodiode voltage at up to 200 kHz through a data acquisition card (DAC).

Figure 3(a) shows the results of an OSNR measurement using a continuous wave signal source. Figure 3(b) shows results obtained with a 10G NRZ-OOK PRBS modulated signal. Figure 4(a) shows the result of adding 600ps/nm of dispersion onto the signal.

Figure 4(b) shows the effect of fully polarized and unpolarised noise on our measurement.

Figure 5(a) shows the results obtained when a poorly biased modulator was used to generate the 10G signal. In Fig. 5(b) and 5(c) the signal was modulated at 2G and 5G respectively.

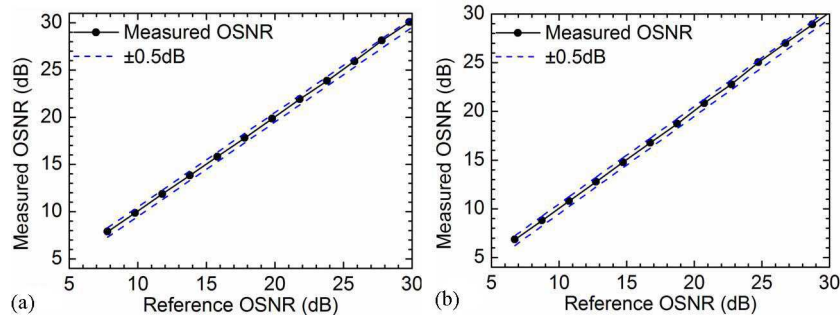


Fig. 3. (a) OSNR measurement using CW source; (b) OSNR measurement using a source modulated at 10G. Outer dashed lines represent an error of ± 0.5 dB.

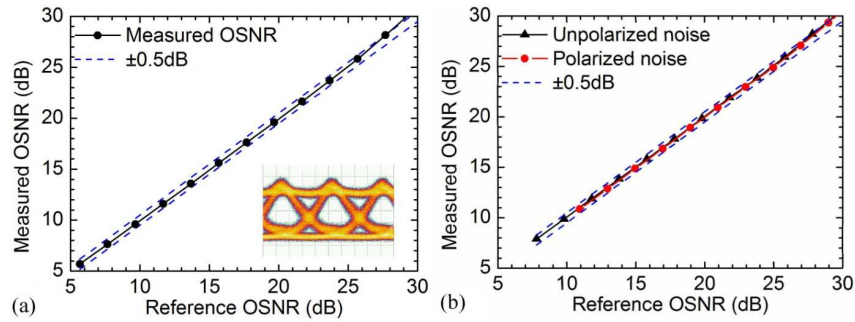


Fig. 4. (a) OSNR measured using a 10G NRZ-OOK signal with 600ps/nm dispersion with the signal eye-diagram shown inset; (b) OSNR results in the case of unpolarised noise and fully polarized noise. Outer dashed lines represent an error of ± 0.5 dB.

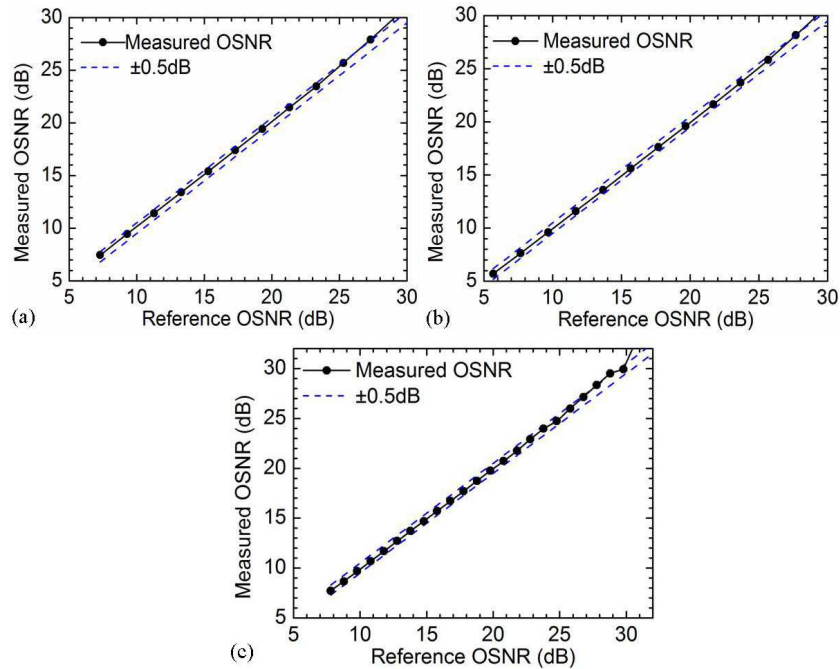


Fig. 5. (a) OSNR results when the MZ modulator used to generate the 10G signal is poorly biased; (b) OSNR monitoring results with a 5G NRZ-OOK signal and (c) a 2G NRZ-OOK. Outer dashed lines represent an error of ± 0.5 dB.

Discussion

It has been shown in Fig. 3(a) and 3(b) that the monitor was capable of measuring OSNR values of up to 30 dB within accuracy of ± 0.5 dB from a noisy CW signal or a 10G NRZ-OOK signal. When 600 ps/nm of dispersion was added, the effect on results was seen to be negligible with a similar measurement range being attained as shown in Fig. 4(a). The effects of fully and partially polarized noise were investigated in Fig. 4(b). This can affect measurement accuracy in both the polarization-nulling method and the orthogonal polarization heterodyne mixing method. In our case, there was little to no effect on measurement accuracy over the measurement range. A poorly biased Mach-Zehnder modulator was employed in the case of Fig. 5(a), the effect of which would be to change $\gamma_s(\tau_d)$ and cause measurement errors if a single interferometer was to be used. Owing to the fact that our system has no reliance on the assumption that $\gamma_s(\tau_d)$ remains constant, a changing $\gamma_s(\tau_d)$

had a minimal effect on the results obtained. It was seen that increasing the bit period to a value much greater than the optical delay by utilizing 2G and 5G NRZ-OOK signal had little effect on the scheme as shown in Fig. 5(b) and 5(c). The optical delay values used in these measurements would not be suitable for use in a 40G system. However, the use of shorter delays should accommodate this with reasonable ease with no further modifications to the setup. The accuracy of the system could be further improved by using detectors with lower noise and larger dynamic range because this can help to measure the extinction ratios of the interferograms more accurately. Another issue is with the parabolic function we have used for γ_s . This approximation is simple and results in linear equations in (16). A more sophisticated approximation may be more accurate but could also be more complex.

Conclusions

We have shown the operation of a new type of OSNR monitor based on two Michelson interferometers with different optical delays under several different modulation speeds up to 10G and under the influence of numerous signal impairments found in optical networks. Unlike other interference based systems, our system is independent of input polarization and requires no dynamic polarization control. It is also immune to the effects of chromatic dispersion, bit rate, poorly biased modulators and polarized noise up to OSNR values of 30 dB and requires no prior knowledge of the signal amplitude autocorrelation function to operate.